Effects of Molecular Structure on Aerosol Yields from OH Radical−Initiated Reactions of Linear, Branched, and Cyclic Alkanes in the Presence of NOx

ARTICLE *in* ENVIRONMENTAL SCIENCE AND TECHNOLOGY · MAY 2009

Impact Factor: 5.33 · DOI: 10.1021/es803389s · Source: PubMed

2 AUTHORS, INCLUDING:

Yong Bin Lim
Korea Institute of Science and Technology
27 PUBLICATIONS **1,047** CITATIONS

SEE PROFILE

Environ. Sci. Technol. **2009,** *43,* 2328–2334

Effects of Molecular Structure on Aerosol Yields from OH Radical-Initiated Reactions of Linear, Branched, and Cyclic Alkanes in the Presence of NO_x

YONG B. LIM[†] AND PAUL J. ZIEMANN*[,‡]

Air Pollution Research Center, University of California, Riverside, California 92521

Received November 30, 2008. Revised manuscript received January 27, 2009. Accepted January 27, 2009.

The effect of hydrocarbon molecular structure on the measured yield and volatility of secondary organic aerosol (SOA) formed from OH radical-initiated reactions of linear, branched, and cyclic alkanes in the presence of NO_x was investigated in an environmental chamber. SOA yields from reactions of homologous series of linear and cyclic alkanes increased monotonically with increasing carbon number due to the decreasing volatility of the parent alkanes and thus the reaction products. For a given carbon number, yields followed the order cyclic > linear > branched, a trend that appears to be determined primarily by the extent to which alkoxy radical intermediates decompose and the nature of the resulting products, with parent alkane volatility being of secondary importance. The trend was investigated quantitatively by correlating SOA yields with the fraction of OH radical reactions that lead to alkoxy radical decomposition (the remainder isomerize), calculated using structure−reactivity relationships. For alkoxy radicals with branched or strained cyclic structures, decomposition can compete with isomerization, whereas for those with linear structures it cannot. Branched alkoxy radicals fragment to form pairs of smaller, more volatile products, whereas cyclic alkoxy radicals undergo ring opening to form products similar to those formed from reactions of linear alkanes, but with an additional aldehyde group. The lower volatility of multifunctional aldehydes, and their tendency to form oligomers, appears to enhance SOA yields.

Introduction

Alkanes are a major component of vehicle emissions and so comprise a large fraction of the pool of non-methane hydrocarbons in urban atmospheres (*1*). In the atmosphere, they react predominantly with OH radicals, at rates corresponding to a lifetime of about 1 day for *n*-decane (*2*). These reactions contribute to the formation of O_3 and a large variety of oxygenated compounds (*2, 3*), including some that can form secondary organic aerosol (SOA) (*4, 5*). The importance of alkanes to atmospheric SOA formation is uncertain, but because recent studies suggest that emissions of large alkanes that can serve as SOA precursors are much higher than previously thought (*6*), the contribution could be significant.

Besides being a potentially important contributor to atmospheric SOA formation, alkanes are an excellent class of compounds for studying the fundamental reactions involved in atmospheric hydrocarbon oxidation and the effects of molecular structure on the formation of low-volatility products that could form SOA. The products of their OH radical-initiated reactions appear to be relatively few in number (*2*−*5*), simplifying data interpretation. In addition, alkanes with a large variety of structures and range of carbon numbers (and therefore volatilities) are available from commercial sources. Here, we focused on laboratory measurements of the yields and volatility of SOA formed from OH radical-initiated reactions of linear, branched, and cyclic alkanes in the presence of NO_x, conditions typical of a polluted atmosphere. We present valuable new data on SOA formation from these reactions. We also demonstrate that most of the fascinating differences observed within and between these three alkane classes can be explained by the effects of alkane molecular structure on the branching ratios for isomerization and decomposition of alkoxy radicals (which along with alkylperoxy radicals are the key reactive intermediates in these systems) and by alkane volatility.

Experimental Section

Chemicals. The following chemicals were used in this study: C_6−C_{17} linear alkanes, C_6−C_8, C_{10}, C_{12}, and C_{15} cyclic alkanes, 2-methylundecane, 2,3-dimethyldecane, 2,6-dimethyldecane, 2,2,4,4-tetramethyloctane, 2,3,6,7-tetramethyloctane, 2,2,4,6,6-pentamethylheptane, 2,3,3-trimethyldecane, 4,4,-dipropylheptane, *n*-butylcyclohexane, 2,6,10-trimethyldodecane, *n*-decylcyclohexane, 3,4-diethylhexane, dioctyl sebacate, and NO. See Table S1 (Supporting Information) for alkane purity and suppliers. Methyl nitrite was synthesized (*7*) and stored in liquid nitrogen.

Environmental Chamber Method. Alkanes were reacted with OH radicals in the presence of NO_x in a 5900 L PTFE environmental chamber filled with clean, dry air (<5 ppbv hydrocarbons, <1% RH) at ~25 °C and atmospheric pressure. The reaction mixture contained ~200−400 μg m^{-3} of dioctyl sebacate (DOS) seed particles added from an evaporation−condensation aerosol generator and 1 (0.5 heptadecane), 10, and 10 ppmv alkane, methyl nitrite, and NO. Reactions were initiated by turning on blacklights to form OH radicals by methyl nitrite photolysis (*8*). The average OH radical concentration for 60 min of reaction was ~3 × 10^7 cm^{-3}, and ~50−85% of the alkane reacted. For the largest linear and cyclic alkanes, SOA mass concentrations were as high as ~6000 μg m^{-3}. Measured alkane, DOS seed particle, and SOA concentrations and the SOA yield for each experiment are given in Table S2 (Supporting Information).

Gas and Particle Measurements. Aerosol volume concentrations were measured using a scanning mobility particle sizer (SMPS) (*9*) comprised of a long differential mobility analyzer, a ^{210}Po bipolar charger, a TSI model 3010 CPC, and software from the McMurry group at the University of Minnesota. The measurements were improved over our previous ones for linear alkanes (*4*) by operating the system with at least 1 L min^{-1} of flow through the charger. For reasons that are not understood, lower flows often gave somewhat lower and less reproducible concentrations. The number and volume concentrations measured with the present system have been determined to be within ±10% of those measured

* Corresponding author phone: (951) 827-5127; fax: (951) 827-5004; e-mail: paul.ziemann@ucr.edu.

[†] Also in the Department of Chemistry. Present address: Department of Environmental Sciences, Rutgers University, New Brunswick, NJ.

[‡] Also in the Departments of Environmental Sciences and of Chemistry.

10.1021/es803389s CCC: $40.75
Published on Web 02/23/2009

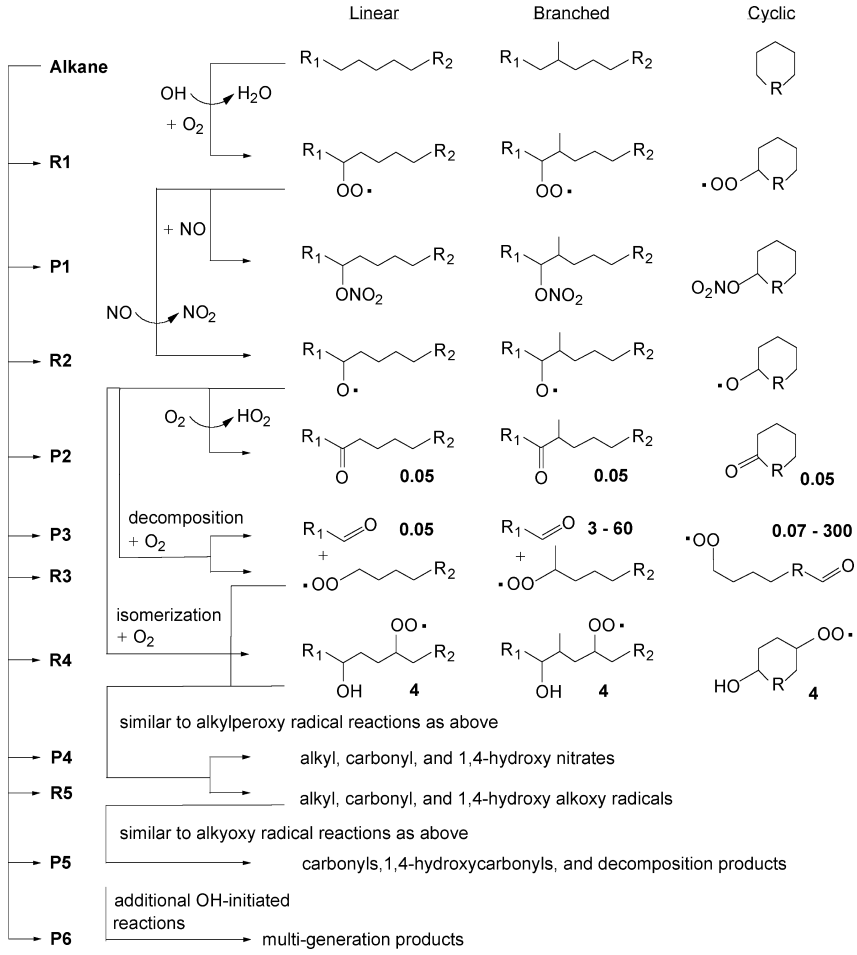

FIGURE 1. Mechanism of OH radical-initiated reactions of alkanes in the presence of NO_x. R, R_1, and R_2 represent alkyl groups, R1−R5 and P1−P6 designate radical intermediates and products, and the bold numbers are typical rate constants (in units of 10^6 s^{-1}) for alkoxy radical reactions with O_2, isomerization, and decomposition.

with a TSI 3936L72 SMPS system and organic aerosol mass concentrations within ±20% of those determined by weighing dried filter extracts (*10*). The aerosol volume concentration was measured throughout the experiment and corrected for particle wall loss using a first-order rate constant (~0.2 h^{-1}) determined from volume concentrations measured for ~30 min after the blacklights were turned off. The SOA mass concentration was calculated by subtracting the initial seed particle volume concentration from the corrected aerosol volume concentration at 60 min and then multiplying by a particle density of 1.06 g cm^{-3}. This value was determined from dried SOA filter extract from the *n*-hexadecane reaction (containing <10% seed aerosol with a density of 0.914 g cm^{-3}): a microliter syringe was weighed, a measured volume of liquid SOA was drawn into the syringe, and then it was reweighed. Alkanes were collected on Tenax TA and analyzed by GC-FID (*11*) to determine the mass of alkane reacted. Concentrations measured for replicate samples taken at 30 min intervals before and after reaction agreed to ±10%, so no corrections were made for wall losses. SOA yields were calculated as SOA mass/reacted alkane mass. A thermal desorption particle beam mass spectrometer was also used to analyze particle composition and volatility by temperature-programmed thermal desorption (TPTD) (*5*). At the end of each experiment, particles were sampled into an aerodynamic lens to form a particle beam that impacted on a polymer-coated metal vaporizer rod cooled to −40 °C. After 30 min of sampling, the rod was allowed to warm to −5 °C and then heated to 200 °C using a 2 °C min^{-1} ramp to desorb and separate compounds by volatility prior to mass analysis using 70 eV electrons and a quadrupole mass spectrometer.

Results and Discussion

Reaction Mechanism and Products. The mechanism of OH radical-initiated reactions of linear, branched, and cyclic alkanes in the presence of NO_x is shown in Figure 1. Detailed discussions are given elsewhere (*2*−*5*). R, R_1, and R_2 represent alkyl groups, and **R1**−**R5** and **P1**−**P6** designate radical intermediates and products. The bold numbers associated with some products correspond to rate constants for the associated alkoxy radical reactions. Reactions are initiated by H-atom abstraction to form alkyl radicals ($R^•$), which add O_2 to form alkylperoxy radicals (**R1**). Reactions with NO then form alkyl nitrates (**P1**) or alkoxy radicals (**R2**), which react with O_2 to form carbonyls (**P2**), decompose, or isomerize. For linear and branched alkanes, decomposition leads to fragmentation and creates two carbonyl (**P3**) plus (after addition of O_2) alkylperoxy radical (**R3**) pairs (one pair shown), whereas for cyclic alkanes a single ring-opened carbonyl alkylperoxy radical (**R3**) is formed. Isomerization of alkoxy radicals followed by addition of O_2 forms 1,4-hydroxy alkylperoxy radicals (**R4**). Alkylperoxy (**R1**), carbonyl alkylperoxy (**R3**), and 1,4-hydroxy alkylperoxy (**R4**) radicals then react with NO to form the corresponding alkyl, carbonyl, and 1,4-hydroxy nitrates (**P4**) and alkoxy radicals (**R5**). Alkyl and carbonyl alkoxy radicals (**R5**) react as described above, while 1,4-hydroxy alkoxy radicals undergo a second, reverse isomerization and react with O_2 to form 1,4-hydroxycarbonyls (**P5**). Though not shown in Figure 1, 1,4-hydroxycarbonyls (**P5**) isomerize rapidly in particles and on walls to cyclic hemiacetals, which can then dehydrate, evaporate, and react again with OH radicals to form additional products. The major

volatile products of alkane reactions are carbonyls, alkyl nitrates, 1,4-hydroxycarbonyls, carbonyl esters, and, for smaller alkanes, 1,4-hydroxy nitrates, all of which can react further with OH radicals to form multigeneration products (**P6**). Under the conditions of these experiments, the formation of multigeneration products and their contributions to SOA formation are substantial, as indicated by detailed analysis of SOA composition (*5*) and modeling (*12*). For example, kinetic modeling indicates that ~50% of first-generation alkyl nitrate products react with OH radicals.

This mechanism can be used to gain insight into the potential effects of alkane molecular structure on SOA formation. The most important reactions for forming SOA are those that lead to multifunctional, low-volatility products that have a greater tendency to condense. They are primarily those that add functional groups while leaving the carbon chain intact. Alkoxy radical isomerization reactions are especially effective at adding functional groups, while multigeneration reactions with OH radicals accomplish similar changes more slowly as long as decomposition is minor. For linear and branched alkanes, alkoxy radical decomposition leads to fragmentation and smaller more volatile products, whereas for cyclic alkanes, it leads to ring-opened alkyl radicals that have an intact carbon chain with an additional aldehyde group, and these can react further to form low-volatility multifunctional products. For acyclic alkanes, it is therefore expected that those that react to form alkoxy radicals that do not decompose will form the most SOA, whereas for cyclic alkanes decomposition may enhance SOA formation. This hypothesis is explored here by using structure−reactivity methods to estimate the fraction of OH radical reactions that lead to alkoxy radical decomposition for alkanes with a variety of structures and correlating these values with measured SOA yields.

Quantification of Alkoxy Radical Decomposition Pathways. The fraction of OH radical reactions with alkanes that lead to alkoxy radical decomposition products were calculated as described in the Supporting Information. They are based on the mechanism shown in Figure 1 and employ structure−reactivity methods of Atkinson and co-workers to calculate rate constants for H-atom abstraction at each carbon atom (*13*) and alkoxy radical rate constants for reactions with O_2, isomerization, and decomposition (*14*). It was also assumed that, for the carbon numbers studied here, alkylperoxy radicals react with NO to form alkoxy radicals with a branching ratio of 0.7 (*15*).

Typical rate constants for alkoxy radical reactions with O_2, isomerization, and decomposition are shown in bold (in units of 10^6 s^{-1}) in Figure 1. Values are ~0.05×10^6 for O_2 reactions (in air at atmospheric pressure) and ~4×10^6 s^{-1} for isomerization (assuming a H atom is available for abstraction and ignoring stearic effects), essentially independent of alkoxy radical structure. For the alkanes studied here, reactions with O_2 are minor. Rate constants for alkoxy radical decomposition are very sensitive to structure, resulting in a large range of values. Most important are the effects of branching and ring strain. Rate constants are lowest for decomposition of linear alkoxy radicals and cyclic alkoxy radicals with no ring strain, ~0.05×10^6 s^{-1}, similar to the O_2 rate constant and much smaller than for isomerization. When the alkoxy radical site is located adjacent to a branch point(s) or is in a ring with significant strain, values are ~2−4 orders of magnitude larger and decomposition competes with isomerization.

SOA Yields. SOA yields measured for reactions of linear, branched, and cyclic alkanes and alkylcyclohexanes are shown in Figure 2 and Tables S1 and S2 (Supporting Information). Yields of linear and cyclic alkanes increase with carbon number, as expected for homologous series of compounds whose reaction products are similar but decrease

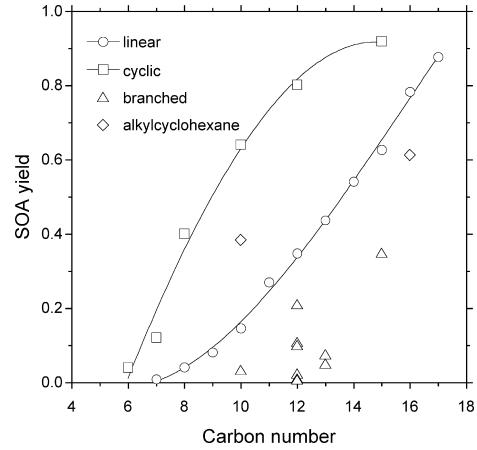

FIGURE 2. Yields of SOA formed from OH radical-initiated reactions of linear, branched, and cyclic alkanes and alkylcyclohexanes in the presence of NO_x.

in volatility with increasing carbon number (as do the parent alkanes), thereby enhancing gas-to-particle partitioning. For any given carbon number, yields follow the order cyclic > linear > branched. Differences in alkane vapor pressures may contribute to this trend by affecting gas−particle partitioning of reaction products, but the effect is probably small. As shown in Figure S1 and Table S1, vapor pressures at 25 °C (P_{25}) of cyclic alkanes are slightly lower than those of the corresponding linear alkanes (equivalent to having ~1 more CH_2 unit), whereas vapor pressures of branched alkanes are slightly higher (equivalent to having ~1 less CH_2 unit). Instead, the ordering of SOA yields most likely is due primarily to differences in alkoxy radical decomposition. Branched alkanes are expected to have lower yields than linear alkanes because of enhanced decomposition that leads to fragmentation and the formation of more volatile products. Cyclic alkanes, especially those with significant ring strain (Table S1), such as the C_7, C_8, C_{10}, and C_{12} compounds, are expected to have higher yields than linear alkanes because enhanced decomposition leads to the formation of less volatile ring-opened products with an additional aldehyde group. The SOA yields of two "mixed-structure" branched alkylcyclohexanes, *n*-butylcyclohexane and *n*-decylcyclohexane, follow no clear trend, with the first falling between the yields of linear and cyclic alkanes and the second falling below the linear alkane yield. It is also worth noting that the yields of SOA formed from reactions of *n*-dodecane and *n*-hexadecane at 50% RH (all others were at <1% RH) were ~30−40% lower than those measured under dry conditions (Tables S1 and S2). This is apparently due to the effect of H_2O on the acid-catalyzed conversion of 1,4-hydroxycarbonyls to dihydrofurans (*5*). Below, we present results of mass spectral analyses and structure−reactivity calculations that provide more detailed and quantitative insights into the factors that influence SOA yields.

Linear Alkanes. The total ion (TI) thermal desorption profiles of SOA formed from reactions of *n*-pentadecane, *n*-dodecane, and *n*-decane are shown in Figure 3A. Because the TI signal is proportional to SOA mass (*16*), these profiles represent the distribution of SOA mass with respect to volatility. It is shown elsewhere (*5*) that the most volatile SOA products formed from the reaction of *n*-pentadecane, which are responsible for the first of the three peaks (the second is actually a shoulder) in the TI profile, are first-generation alkyl nitrates and 1,4-hydroxy nitrates. The next two peaks are associated with less volatile multigeneration products. As the alkane carbon number decreases, in the present case from 15 to 12 to 10, product peaks shift to lower desorption temperatures because of their increased volatility. For alkyl nitrates and 1,4-hydroxy nitrates, the increase in

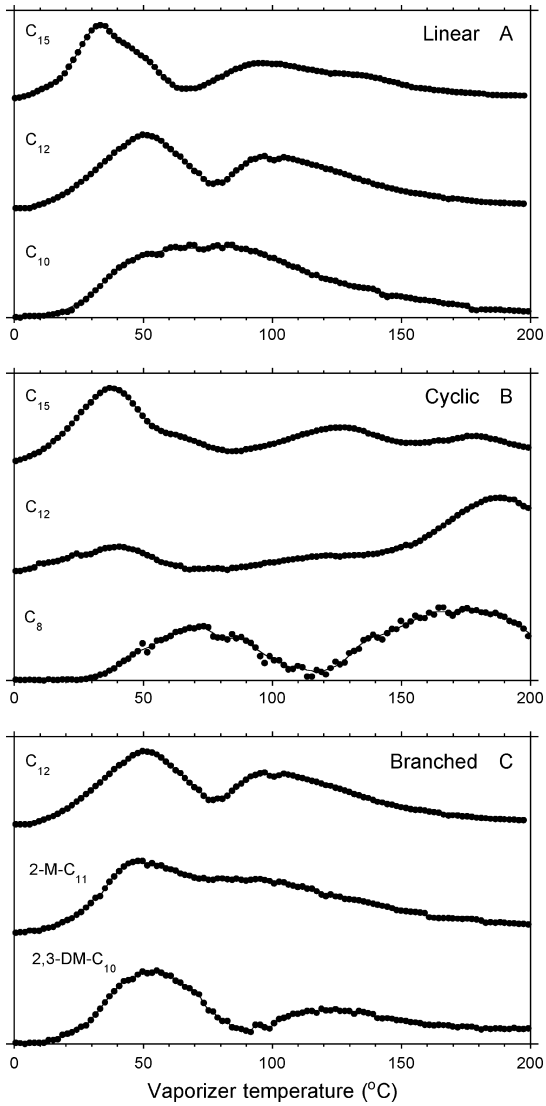

FIGURE 3. Total ion thermal desorption profiles of SOA formed from OH radical-initiated reactions of (A) linear, (B) cyclic, and (C) branched alkanes in the presence of NO_x. Signals were normalized so that the largest peak in each profile has the same intensity. C_{15}, C_{12}, and C_{10} linear alkanes are *n*-pentadecane, *n*-dodecane, and *n*-decane, the C_{15}, C_{12}, and C_8 cyclic alkanes are cyclopentadecane, cyclododecane, and cyclooctane, and the C_{12}, 2-M-C_{11}, 2,3-DM-C_{10} branched alkanes are *n*-dodecane, 2-methylundecane, and 2,3-dimethyldecane.

volatility is sufficient that they do not form SOA in the reaction of *n*-dodecane, thereby resulting in a TI profile with only two peaks, both of which are due to multigeneration products. In the reaction of *n*-decane, some of the multigeneration products are also too volatile to form SOA, so only a single peak is observed. The SOA is then comprised entirely of low-volatility multigeneration products corresponding to those that desorb above ~75 °C in the *n*-dodecane and *n*-pentadecane TI profiles. The magnitude of the shift in desorption temperature with alkane carbon number is fairly regular for first-generation products, as indicated by the disappearance of alkyl nitrates and 1,4-hydroxy nitrates between *n*-pentadecane and *n*-dodecane (and data for other *n*-alkanes not shown here), but is less so for multigeneration products. For example, a peak is present at ~100 °C for *n*-pentadecane and *n*-dodecane, but shifts to ~75 °C for *n*-decane. This may be due to the nature of the multigeneration products, many of which contain a cyclic hemiacetal unit that may form oligomers (*5*). The progressive increase in the volatility of reaction products with decreasing carbon number, which reduces their tendency to form SOA, results in a progressive decrease in the yields of SOA formed from the reactions of *n*-pentadecane, *n*-dodecane, and *n*-decane from 0.63 to 0.35 to 0.15.

Cyclic Alkanes. The TI thermal desorption profiles of SOA formed from reactions of cyclopentadecane, cyclododecane, and cyclooctane are shown in Figure 3B. The profile for cyclopentadecane is similar to that for *n*-pentadecane, as is the SOA mass spectrum (*5*), indicating that the products are similar. This is reasonable. Since cyclopentadecane apparently has little or no ring strain, the cyclic alkoxy radicals decompose very little (Table S1, Supporting Information), similar to linear alkoxy radicals. The same reaction pathways are therefore expected to dominate product formation in these two systems. As the size of the alkane ring decreases, however, interesting differences appear in the desorption profiles. The most obvious is that the contribution of low-volatility products to SOA mass increases, with a large peak growing in above ~150 °C. The likely reason for this is that cyclododecane and cyclooctane have significant ring strain, enhancing alkoxy radical decomposition and the formation of a substantial fraction of multifunctional ring-opened products. These products contain an aldehyde group, which will lower the volatility of the products relative to those formed from linear alkanes. Aldehydes can also form oligomers, such as hemiacetals (*17*). The thermal desorption particle beam mass spectrometry (TDPBMS) spectra obtained in our studies (*5*) do not show evidence of oligomers, but this does not preclude their presence since they often decompose during thermal desorption/electron ionization (*11*). In our experience, only high molecular weight oligomers would desorb at these very high temperatures, which correspond to vapor pressures of less than $\sim 10^{-13}$ Pa (*5*).

The effect of a ring on SOA yields from cyclic alkanes can be quantified in a number of different ways. One is to compare the yields with those from linear alkanes with the same carbon number. Alternatively, one can compare the carbon numbers of linear and cyclic alkanes with the same yield. For the data presented here, the latter approach is better. This is because to compare differences in yields across the entire range of carbon numbers, it is necessary to calculate relative differences, such as Δyield/average yield. At small carbon numbers, however, where the yields are small (approaching 0) and similar in magnitude to the measurement uncertainties, this value is very sensitive to errors and highly uncertain. Conversely, the range of differences in carbon numbers between linear and cyclic alkanes with the same yield is about 1−5 and can be directly compared. This approach is taken below.

Figure 4A shows the same SOA yield data shown in Figure 2 for linear [LA(meas)] and cyclic [CA(meas)] alkanes, but plotted as carbon number vs SOA yield. CA(calc P_{25}) is a plot of carbon number vs SOA yield calculated using cyclic alkane P_{25} values and the least-squares fit to a plot of SOA yield vs log P_{25} for linear alkanes shown in Figure S3 (Supporting Information). It is the plot expected for cyclic alkanes if the products are similar to those formed from linear alkanes and the yields are primarily determined by the vapor pressures of the parent alkanes. It serves as a reference for comparing the effects of alkoxy radical decomposition on SOA formation, since decomposition is negligible for linear alkanes. One can think of the CA(calc P_{25}) plot as being shifted to the right of the linear alkane plot because the lower vapor pressures of cyclic alkanes should result in higher SOA yields. Alternatively, it can be thought of as being shifted downward by about 1 carbon number, meaning the yield calculated for a C_n cyclic alkane is approximately the same as that of a C_{n+1} linear alkane. As shown in Figure S1, this shift is due to a factor of

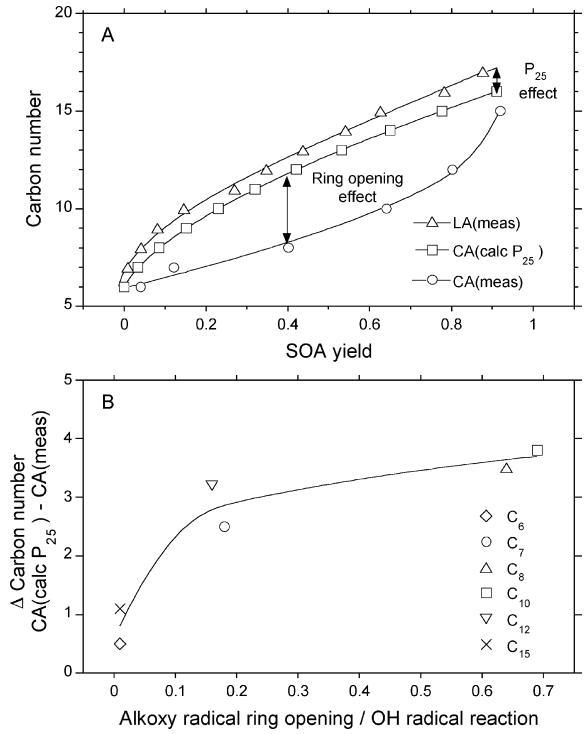

FIGURE 4. (A) Effects of vapor pressure and ring opening on yields of SOA formed from OH radical-initiated reactions of cyclic alkanes in the presence of NO_x, determined by comparing carbon numbers of alkanes with the same yield. Plots were created using the carbon number dependence of SOA yields measured for linear [LA(meas)] and cyclic [CA(meas)] alkanes and calculated [CA(calc P_{25})] using cyclic alkane P_{25} values and the least-squares fit to a plot of SOA yield vs log P_{25} for linear alkanes. (B) Relationship between the difference in carbon number attributed to alkoxy radical ring opening and the fraction of OH radical reactions calculated to lead to ring-opened products.

~3 lower vapor pressure for cyclic alkanes compared to linear alkanes with the same carbon number.

The differences in SOA yields measured and calculated for cyclic alkanes provide a quantitative estimate of the effect of alkoxy radical decomposition on yields, since the effect of the parent alkane vapor pressure on the volatility of reaction products is presumably accounted for in CA(calc P_{25}) values. As shown in Figure 4A, the carbon number differences are less than ~1 for the smallest and largest alkanes, cyclohexane and cyclopentadecane, but increase to ~3−4 for the intermediate sizes, cyclooctane and cylcodecane. In Figure 4B, these differences are plotted vs the fractions of OH radical reactions calculated to lead to ring-opened products by alkoxy radical decomposition, which are given in Table S1 (Supporting Information). As expected, the fractions are strongly correlated with alkane ring strain, as shown in Figure S2. They increase from ~0 for C_6 and C_{15} to ~0.2 for C_7 and C_{12} and then to a maximum of ~0.7 for C_8 and C_{10}. The plot in Figure 4B clearly indicates that ring-opened products increase the yields of SOA formed from reactions of cyclic alkanes. The largest effect occurs between a fraction of ring-opened products of 0, which is the value for linear alkanes, and ~0.2, where the effect on SOA yields is equivalent to adding ~3 CH_2 units to the parent alkane and thereby reducing the vapor pressure by a factor of ~30. Increasing the fraction beyond this value has little additional effect, indicating that a relatively small fraction of these products can have a large and saturating effect on SOA formation.

It is worth discussing further the observation that the carbon number differences for C_6 and C_{15} in Figure 4 are slightly greater than 0, which lends some uncertainty to our estimates of the effects of ring opening on SOA yields. One possibility is that this is mostly due to measurement uncertainty. For example, the SOA yields calculated and measured for the reaction of cyclopentadecane are 0.78 and 0.92, values that differ by less than 10% from their mean of 0.85. If the discrepancy is not due to this, then it indicates that our method for calculating SOA yields using P_{25} values does not completely capture the effects of molecular structure. The simplest explanation is that the vapor pressures of the products do not scale by the same factors as those of the parent alkanes, as is assumed in the calculations, and that the ring-retaining products are less volatile and so form more SOA than predicted. Alternatively, it could be that the fraction of ring-opened products formed from the reaction of cyclopentadecane is slightly larger than was calculated, which is not unreasonable since the value of 0 used for ring strain in the calculation is not as firmly established for cylcopentadecane as it is for cyclohexane. The small peak at ~180 °C in the cyclopentadecane TI profile lends support to this explanation. Large peaks are present at this temperature in the cyclododecane and cyclooctane profiles, ascribed here to ring-opened products, whereas none are present in the *n*-pentadecane profile. Depending on which of these explanations is correct, the carbon number differences in Figure 4B might be too high by ~0.5−1.

Branched Alkanes. The TI thermal desorption profiles of SOA formed from reactions of two branched C_{12} alkanes, 2-methylundecane and 2,3-dimethyldecane, are shown in Figure 3C with that of *n*-dodecane, the linear C_{12} alkane. All three profiles have peaks at ~50 and ~80−150 °C, indicating the SOA products of reactions of linear and branched alkanes are similar, a conclusion that is consistent with their mass spectra (*5*). In spite of the similarities in SOA composition and volatility, however, the yields decrease in the order *n*-dodecane > 2-methylundecane > 2,3-dimethyldecane from 0.35 to 0.21 to 0.11. These observations are consistent with the expectation that alkoxy radical decomposition increases with branching, enhancing the formation of smaller, more volatile fragmentation products that form less SOA than those formed from linear alkanes with the same carbon number. The major SOA products will be formed through isomerization pathways and multiple generations of OH reactions and therefore will be similar in identity but different in quantity. Figure 5A shows the trend in SOA yields for the C_{12} alkanes in Table S1 (Supporting Information), which range from *n*-dodecane, with no branching methyl groups, to 2,2,4,6,6-pentamethylheptane, with five. The effect is dramatic; yields decrease monotonically with increased branching, with 4−5 branching methyl groups reducing the yield from 0.35 to almost 0.

The effects of alkoxy radical decomposition on SOA yields from reactions of branched alkanes can be explored in more detail using an approach similar to that used above for cyclic alkanes, again using linear alkanes as a reference. BA(calc P_{25}) carbon numbers were obtained by first calculating SOA yields using branched alkane P_{25} values and the least-squares fit to a plot of SOA yield vs log P_{25} for linear alkanes shown in Figure S3 (Supporting Information). These yields and those measured for C_{12} branched alkanes were then used with the least-squares fit to the LA(meas) plot in Figure 4A (also shown in Figure S4 with the equation) to calculate BA(calc P_{25}) and BA(calc yield) carbon numbers, respectively. These carbon numbers correspond to those of linear alkanes with the same P_{25} values and SOA yields as the branched alkanes. The results of these calculations are presented in Figure 5B, as plots of carbon number vs branching methyl groups, with the plot for a C_{12} linear alkane included as a reference. The carbon numbers calculated using P_{25} values decrease relative to that of the C_{12} linear alkane at a rate of ~0.35 per branching methyl

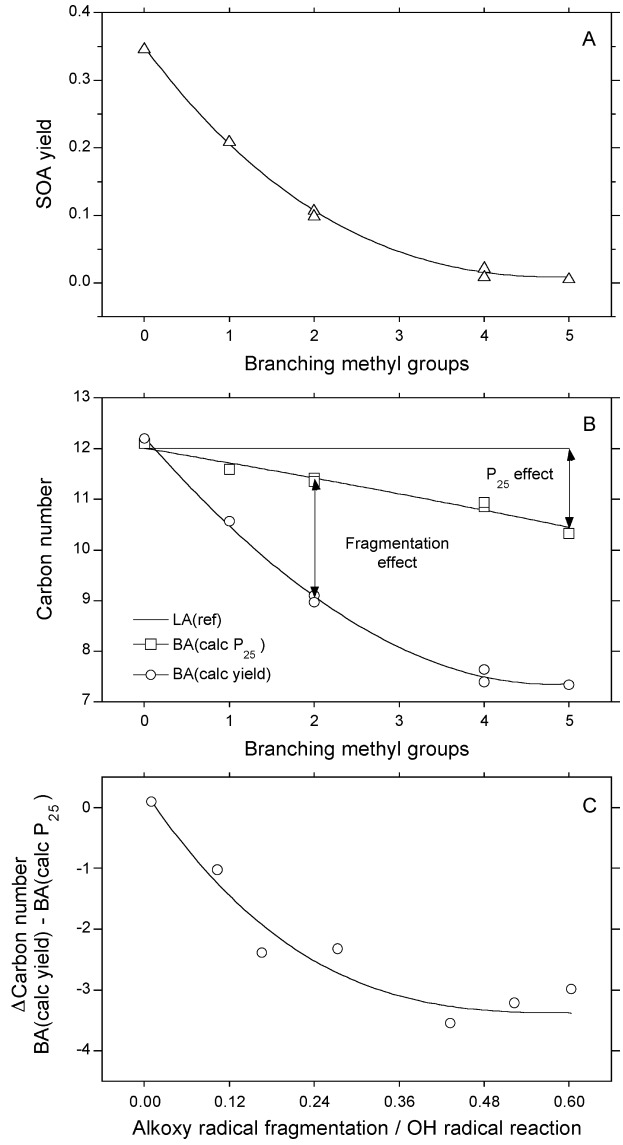

FIGURE 5. (A) Effect of chain branching on yields of SOA formed from OH radical-initiated reactions of C_{12} branched alkanes in the presence of NO_x. (B) Effects of vapor pressure and alkoxy radical fragmentation on SOA yields, determined by comparing carbon numbers of alkanes with the same yield. Carbon numbers were calculated using the least-squares fit to the LA(meas) plot in Figure 4A with yields measured [BA(calc yield)] and calculated [BA(calc P_{25})] for branched alkanes. The calculated SOA yields were calculated using branched alkane P_{25} values and the least-squares fit to a plot of SOA yield vs log P_{25} for linear alkanes. The LA(ref) plot is for a C_{12} linear alkane, included as a reference. (C) Relationship between the difference in carbon number attributed to alkoxy radical fragmentation and the fraction of OH radical reactions calculated to lead to fragmentation products.

group, due to an increase in the vapor pressures of C_{12} branched alkanes by a factor of ~1.6 per branching methyl group. The carbon numbers calculated using SOA yields decrease much faster, at an average rate of ~1 per branching methyl group, due to the added effects of alkoxy radical decomposition on reaction products.

In Figure 5C, the differences between carbon numbers calculated using SOA yields and P_{25} values are plotted vs the fractions of OH radical reactions calculated to lead to ring-opened products by alkoxy radical decomposition, which are given in Table S1 (Supporting Information). The plot clearly indicates that fragmentation of alkoxy radicals decreases the yields of SOA formed from reactions of branched alkanes. The plot levels off more slowly than was observed for cyclic alkanes, reaching a plateau where the yields correspond to those of linear alkanes with ~3–4 fewer CH_2 groups in the carbon chain. This occurs when the fractions of OH radical reactions calculated to lead to fragmentation are greater than ~0.4. For these alkanes, the latter quantity is linearly proportional to the number of branching methyl groups (0.12 per branching methyl group, as shown in Figure S5), so the plateau is also the point at which at least four branching methyl groups are present. As shown by the BA(calc yield) curve in Figure 5B, the SOA yields of these C_{12} branched alkanes are approximately the same as those of linear alkanes with carbon numbers equal to 12 minus the number of branching methyl groups.

Application of Results to the Atmosphere. An important consideration for laboratory studies of SOA formation is whether, or how, results can be applied to the atmosphere, especially for modeling purposes. For SOA yields, the most common approach is to carry out experiments under conditions that attempt to mimic the atmosphere, using a range of initial hydrocarbon concentrations (to produce different amounts of SOA), possibly while varying other quantities such as NO_x, RH, or seed particle properties (*18*). The measured yields are then parametrized as a function of organic mass concentration for use in models. The purpose of the present study was not to measure yields that could be used directly in models, so much higher alkane, NO_x, and particle mass concentrations were employed in experiments than are found in the atmosphere. This was done to improve the accuracy of SOA yield measurements, expand the range of alkanes over which trends could be measured, and generate sufficient aerosol for TDPBMS analysis even when SOA yields were small. The results provide interesting and important new insights into the effects of hydrocarbon molecular structure on reaction mechanisms and products, information that is necessary for understanding in detail the process of SOA formation. Without such knowledge it is difficult to apply with confidence the results of any laboratory experiment to the atmosphere.

The general trends in SOA yields observed here were cyclic > linear > branched for a given alkane carbon number, with values increasing with increasing carbon number within a particular alkane class; they are likely to be similar under atmospheric conditions. Quantities such as NO_x, O_3, organic aerosol mass and composition, and particle acidity can impact some aspects of the reaction mechanism and products (*5, 18*), but the branching ratios for alkoxy radical isomerization and decomposition will be the same. The effects of alkane molecular structure and carbon number on the composition and volatility of products, and thus the trends in SOA yields, are therefore expected to be similar for a large range of conditions. The magnitudes of the yields, however, are likely to be lower in the atmosphere, due primarily to reductions in gas-to-particle partitioning of semivolatile products, including precursors to oligomer formation, at lower particle mass concentrations. Left in the gas phase, these products will react further to form (at least in part) more oxidized and less volatile multigeneration products that might then partition to the particle phase. The results reported here can provide guidance for predicting the relative importance of different alkane classes to atmospheric SOA formation, but measurements of SOA yields at low ppbv concentrations of alkanes would be helpful. The effects of quantities such as NO_x, O_3, and particle acidity should also be explored. Although the yields measured here cannot be directly applied to the atmosphere, they can be used to evaluate detailed physical-chemical models developed for simulating SOA formation, and these can then be employed under atmospheric conditions. The SOA yields presented

here for linear alkanes were recently used to evaluate such a model (*12*).

Acknowledgments

This material is based on work supported by the National Science Foundation (NSF) under Grants ATM-0234586 and ATM-0650061. Any opinions, findings, and conclusions or recommendations expressed in this material are those of the authors and do not necessarily reflect the views of the NSF. We thank Roger Atkinson for helpful discussions.

Supporting Information Available

Calculation method used to quantify alkoxy radical decomposition pathways, Table S1 giving alkane vapor pressures, ring strain energies, calculated fractions of OH radical reactions that lead to alkoxy radical decomposition, and average SOA yields, Table S2 giving measured alkane, DOS seed particle, and SOA concentrations and the SOA yield for each experiment, Figure S1 showing the relationships between vapor pressure and alkane carbon number, Figure S2 showing the relationship between alkoxy radical ring opening/OH radical reaction and ring strain for cyclic alkanes, Figure S3 showing the relationship between SOA yield and vapor pressure for linear alkanes, Figure S4 showing the relationship between carbon number and SOA yield for linear alkanes, and Figure S5 showing the relationship between alkoxy radical fragmentation and branching methyl groups for C_{12} alkanes. This material is available free of charge via the Internet at http://pubs.acs.org.

Literature Cited

(1) Calvert, J. G.; Atkinson, R.; Kerr, J. A.; Madronich, S.; Moortgat, G. K.; Wallington, T. J.; Yarwood, G. *The Mechanisms of Atmospheric Oxidation of the Alkenes*; Oxford University Press: Oxford, U.K., 2000.

(2) Atkinson, R.; Arey, J. Atmospheric degradation of volatile organic compounds. *Chem. Rev.* **2003**, *103*, 4605–4638.

(3) Atkinson, R.; Arey, J.; Aschmann, S. M. Atmospheric chemistry of alkanes: Review and recent developments. *Atmos. Environ.* **2008**, *42*, 5859–5871.

(4) Lim, Y. B.; Ziemann, P. J. Products and mechanism of secondary organic aerosol formation from reactions of *n*-alkanes with OH radicals in the presence of NO_x. *Environ. Sci. Technol.* **2005**, *39*, 9229–9236.

(5) Lim, Y. B.; Ziemann, P. J. Chemistry of secondary organic aerosol formation from OH radical-initiated reactions of linear, branched, and cyclic alkanes in the presence of NO_x. *Aerosol Sci. Technol.*, in press.

(6) Robinson, A. L.; Donahue, N. M.; Shrivastava, M. K.; Weitkamp, E. A.; Sage, A. M.; Grieshop, A. P.; Lane, T. E.; Pierce, J. R.; Pandis, S. N. Rethinking organic aerosols: Semivolatile emissions and photochemical aging. *Science* **2007**, *315*, 1259–1262.

(7) Taylor, W. D.; Allston, T. D.; Moscato, M. J.; Fazekas, G. B.; Kozlowski, R.; Takacs, G. A. Atmospheric photodissociation lifetimes for nitromethane, methyl nitrite, and methyl nitrate. *Int. J. Chem. Kinet.* **1980**, *12*, 231–240.

(8) Atkinson, R.; Carter, W. P. L.; Winer, A. M.; Pitts, J. N., Jr. An experimental protocol for the determination of OH radical rate constants with organics using methyl nitrite photolysis as an OH radical source. *Air Pollut. Control Assoc.* **1981**, *31*, 1090–1092.

(9) Wang, S. C.; Flagan, R. C. Scanning electrical mobility spectrometer. *Aerosol Sci. Technol.* **1990**, *13*, 230–240.

(10) Matsunaga, A.; Docherty, K. S.; Lim, Y. B.; Ziemann, P. J. Composition and yields of secondary organic aerosol formed from OH radical-initiated reactions of linear alkenes in the presence of NO_x: Modeling and measurements. *Atmos. Environ.* **2009**, *43*, 1349–1357.

(11) Docherty, K. S.; Wu, W.; Lim, Y. B.; Ziemann, P. J. Contributions of organic peroxides to secondary aerosol formed from reactions of monoterpenes with O_3. *Environ. Sci. Technol.* **2005**, *39*, 4049–4059.

(12) Jordan, C. E.; Ziemann, P. J.; Griffin, R. J.; Lim, Y. B.; Atkinson, R.; Arey, J. Modeling SOA formation from OH reactions with C_8-C_{17} *n*-alkanes. *Atmos. Environ.* **2008**, *42*, 8015–8026.

(13) Kwok, E. S. C.; Atkinson, R. Estimation of hydroxyl radical reaction rate constants for gas phase organic compounds using a structure-reactivity relationship: An update. *Atmos. Environ.* **1995**, *29*, 1685–1695.

(14) Atkinson, R. Rate constants for the atmospheric reactions of alkoxy radicals: An updated estimation method. *Atmos. Environ.* **2007**, *41*, 8468–8485.

(15) Arey, J.; Aschmann, S. M.; Kwok, E. S. C.; Atkinson, R. Alkyl nitrate, hydroxyalkyl nitrate, and hydroxycarbonyl formation from the NO_x-air photooxidations of C_5-C_8 *n*-alkanes. *J. Phys. Chem. A* **2001**, *105*, 1020–1027.

(16) Crable, G. F.; Coggeshall, N. D. Application of total ionization principles to mass spectrometric analysis. *Anal. Chem.* **1958**, *30*, 310–313.

(17) Jang, M.; Czoschke, N. M.; Lee, S.; Kamens, R. M. Heterogeneous atmospheric aerosol production by acid-catalyzed particle-phase reactions. *Science* **2002**, *298*, 814–817.

(18) Kroll, J. H.; Seinfeld, J. H. Chemistry of secondary organic aerosol: Formation and evolution of low-volatility organics in the atmosphere. *Atmos. Environ.* **2008**, *42*, 3593–3624.

ES803389S